EPR Studies of the Dynamics of Rotation of Dioxygen in Model Cobalt(II) Hemes and Cobalt-Containing Hybrid Hemoglobins

ARTICLE *in* THE JOURNAL OF PHYSICAL CHEMISTRY B · OCTOBER 1997

Impact Factor: 3.3 · DOI: 10.1021/jp9711306

5 AUTHORS, INCLUDING:

Arnold M Raitsimring
The University of Arizona
126 PUBLICATIONS **2,632** CITATIONS
SEE PROFILE

Daniel H Buttlaire
San Francisco State University
18 PUBLICATIONS **391** CITATIONS
SEE PROFILE

F(rances) Ann Walker
The University of Arizona
242 PUBLICATIONS **8,718** CITATIONS
SEE PROFILE

EPR Studies of the Dynamics of Rotation of Dioxygen in Model Cobalt(II) Hemes and Cobalt-Containing Hybrid Hemoglobins

James H. Bowen,[†] Nikolai V. Shokhirev,[‡] Arnold M. Raitsimring,[‡] Daniel H. Buttlaire,[†] and F. Ann Walker*[,‡]

Department of Chemistry and Biochemistry, San Francisco State University, San Francisco, California 94132, and Department of Chemistry, University of Arizona, Tucson, Arizona 85721

Received: March 31, 1997; In Final Form: July 28, 1997[⊗]

Earlier we showed that the shapes of the EPR spectra of cobalt(II) porphyrinate(nitrogen base)(dioxygen) complexes in fluid solution were sensitive to the rate of rotation about the Co−O bond (Walker, F. A.; Bowen, J. H. *J. Am. Chem. Soc.* **1985**, *107*, 7632). We have now extended these studies to four metal-substituted hybrid hemoglobins in an attempt to determine whether EPR spectroscopy is sensitive to differences in the mobility of dioxygen in the α and β subunits of the T and R quaternary states. For purposes of this study, $[\alpha_2(CoO_2)\beta_2(FeO_2)]$ and $[\alpha_2(FeO_2)\beta_2(CoO_2)]$ were used as R-state models and $[\alpha_2(CoO_2)\beta_2(Zn)]$ and $[\alpha_2(Zn)\beta_2(CoO_2)]$ were used as T-state models. EPR spectra were recorded for samples of each of the above hybrids, equilibrated with 1 atm of O_2 gas, as a function of temperature. The "progress toward averaging" of the EPR signals of the Co−O_2-containing subunits was measured as the difference in field positions, ΔH, for the midpoint of the low- and high-field extrema of the derivative EPR spectra. A plot of ΔH vs temperature for each hybrid shows that the $[\alpha_2(Zn)\beta_2(CoO_2)]$ hybrid is unique in averaging more slowly than the other three (all of which behave similarly), indicating more restricted rotation of dioxygen in T-state β-chain pockets than in the heme distal O_2-binding pockets of any other form. This finding is consistent with X-ray crystallographic data which show that valine E11 on the distal side of the T-state β-chain pocket partially blocks the dioxygen binding site (Perutz, M. F.; Fermi, G.; Luisi, B.; Shaanan, B.; Liddington, R. C. *Acc. Chem. Res.* **1987**, *20*, 309). Simulation of EPR spectra as a function of jump time provides semiquantitative estimates of the rate of dioxygen rotation in these mixed-metal hemoglobin−dioxygen samples; these rates are in the 1×10^8 s^{-1} range for three of the hybrids at 35−37 °C, and about one-third that value for T-state $\beta(CoO_2)$ centers. These results provide new insight into the highly dynamic nature of dioxygen bound to the metal centers of hemoglobin at physiological temperatures.

Introduction

Since the report of the crystal and molecular structure of the tetrameric heme protein methemoglobin by Perutz and co-workers in 1968,[1] there have been a number of further structural studies that have provided detailed insight into the structural basis for the cooperativity of binding of dioxygen that has been observed in the kinetics and equilibria of dioxygen binding and release[2−5] for many years. The two-state allosteric mechanism originally proposed by Monod and co-workers[6] was first interpreted in terms of a structural model by Perutz in 1970[7] and has been elaborated and extended several times since.[8,9] The two states are described as the deoxy or "tense" (T) form and the oxy or "relaxed" (R) form, and each form has a distinct 3-dimensional structure. The dioxygen binding affinity of the T structure is slightly less than that of the R structure.[9] The T and R structures differ in the relationship of the four subunits (two α and two β chains, each of which contains a protoheme molecule that can bind one molecule of O_2) to each other, as well as in the conformation of the individual subunits. The quaternary T→R transition causes a rotation of one $\alpha\beta$ dimer relative to the other by 12−15° and a translation of one dimer relative to the other by about 0.8 Å.[9] Binding of O_2 to the α subunits in crystals of deoxyhemoglobin causes movement of the α-chain Fe atoms toward the porphyrin by 0.15 Å, though the porphyrin remains domed, and approximately 30% of the hemes in the β-chains of the crystals studied were oxidized to the inactive *met* form.[9] In the T state, the crystal structures have shown that the distal valine E11 obstructs the binding site for O_2 in the β-chain hemes.[9] From this and many studies of the kinetics of dioxygen binding, the impression has arisen that O_2 binds more readily to the α-chain than to the β-chain hemes. This is an oversimplification, however, as pointed out by the detailed studies of Ackers et al.,[5] who find that of the eight *partially* ligated states of hemoglobin, quaternary switching from T to R occurs whenever binding to the hemes creates a tetramer with at least one ligated subunit on each dimeric half-molecule. Recent use of the Laue method, coupled with fast laser flashes to break the Fe−CO bond, have allowed visualizing the Fe out-of-plane, histidine and protein chain movements that occur on very short time scales when CO is flashed off the heme centers of crystals of the related monomeric protein, myoglobin.[10,11]

Metal-substituted hemoglobins, especially the "hybrid" hemoglobins having different metals (or different oxidation states of the same metal) in the porphyrin rings of α and β subunits, have been extremely useful in obtaining detailed information concerning cooperativity in the binding of dioxygen (and other ligands) to hemoglobin. Dynamic properties, spectroscopic signatures and static structures have been studied for a large number of metal-substituted hemoglobins and myoglobins.[12] For these techniques to be used, methods had to be developed for preparation of the mixed-metal proteins in pure form. Yonetani[13] used the acid−butanone method first reported by Teale[14] to show that hemin could be removed from both cytochrome *c* peroxidase and methemoglobin by this method, and that the

[†] San Francisco State University.
[‡] University of Arizona.
[⊗] Abstract published in *Advance ACS Abstracts,* October 1, 1997.

S1089-5647(97)01130-9 CCC: $14.00

former protein in tris-HCl buffer at pH 8.0 could be reconstituted with hemin dissolved in 0.1 M NaOH.[13] Shortly thereafter, the first reports of the oxygen binding characteristics of hybrid hemoglobins having one type of subunit in the cyanomet form[15,16] or simply mixed oxidation state hybrid hemoglobins[17] were reported, and not long after those reports, Waterman and Yonetani reported the first mixed metal hybrid hemoglobins, the $[\alpha_2(FeCO)\beta_2(Mn^{3+})]$ and $[\alpha_2(Mn^{3+})\beta_2(FeCO)]$ hybrids.[18] At about the same time, Hoffman and Petering[19] reported the preparation of "coboglobins", the cobalt−protoporphyrin complexes of myoglobin and hemoglobin, and showed that they bind O_2 reversibly. (Hoffman has since reviewed the preparation and study of metal-substituted hybrid hemoglobins.[12]) Because of the odd-electron configuration of Co(II) (d^7), the dioxygen complex is EPR-active, while the Fe(II)−O_2 center is not. Hence, EPR spectroscopy could be used to investigate questions related to the effects of the allosteric mechanism of O_2 binding, although mixed-metal Co, Fe hybrid hemoglobins were not reported until 1977.[20] Single-crystal EPR spectroscopy of the dioxygen complex of cobalt(II)-containing myoglobin[21−24] and its deoxy precursor[25] have been reported. In addition, EPR spectra of Co,Fe hybrids of hemoglobin show that there are slight differences in the EPR spectra of the Co−O_2 centers of the T- and R-state forms of oxyhemoglobin.[26]

We were among the first investigators to study the EPR spectrum of synthetic porphyrinatocobalt(II)−dioxygen complexes in detail,[27] and we have extended these studies over the years to investigate the equilibrium constants for binding dioxygen to 5-coordinate cobalt porphyrinates,[28] the effect of organic π-complexing agents on the Co−O_2 EPR spectral parameters,[29] the relationship between equilibrium constants for binding dioxygen and the Co^{III}/Co^{II} reduction potentials of a series of 5-coordinate cobalt porphyrinates[30] and the effect of hydrogen-bonding from a porphyrin substituent to the terminal oxygen atom of coordinated O_2 on the dynamics of rotation of dioxygen about the Co−O bond.[31] In the latter work striking differences in the shape of the EPR signal were observed for two monoacetamide ($NHCOCH_3$) substituted TPPCo(*N*-MeIm)-(O_2) complexes as a function of temperature: The mono-*p*-$NHCOCH_3$ derivative, like all other Co(II) porphyrinates studied previously, exhibits a rhombic, powder-type spectrum having at least 17 resolved lines below the freezing point of the solvent (toluene, −95 °C), while it exhibits an "isotropic" 8-line EPR signal above the freezing point of the solvent.[31] In comparison, the mono-*o*-$NHCOCH_3$ derivative exhibits a quite different temperature-dependent behavior, in which the same rhombic, powder-type EPR spectrum is observed below the freezing point of the solvent, but above −95 °C the EPR spectrum first loses the ^{59}Co hyperfine structure and then slowly broadens further, with the outermost "wings" of the spectrum slowly moving toward the center (as shown on the right-hand side of Figure 1 of ref 31). Only near room temperature, where, unfortunately, the dioxygen complex is not very stable, does the eight-line "isotropic" spectral pattern develop.[31] We interpreted this behavior as being due to slow rotation of the dioxygen moiety due to hydrogen-bonding between the amide N−H proton and the terminal O of the coordinated O_2,[31] which is bound at a Co−O−O angle of approximately 145°.[32,33]

In that same study we also extended our investigation from synthetic cobalt(II) tetraphenylporphyrinates to the dioxygen complex of cobalt-substituted myoglobin, $CoMbO_2$, and showed that a similar loss of hyperfine structure, followed by slow collapse of the rhombic signal occurs in this case as well.[31] (A detailed report of these spectral changes for $CoMbO_2$ had appeared earlier,[24] but the authors had not recognized the reason for the changes.) Hence, it was clear to us that the rotation of dioxygen in the heme pocket of $CoMbO_2$ is hindered (either due to H-bonding between the distal histidine and O_2 or to crowding of distal pocket protein residues against the bound O_2) that the rates of rotation of dioxygen are slow but measurable on the EPR time scale, and that the rate of rotation might be measureable by EPR line-shape analysis techniques. We thus decided to extend our studies to Co-substituted hemoglobins, for which, by proper choice of partner metals, we could stabilize the T or R quaternary state and attempt to discover whether there were differences in the rate of rotation of bound O_2 in the α and β subunits in the two different quaternary states. Although the experimental work reported herein was completed some time ago,[34] they have not previously been published in the formal scientific literature, and methods for analyzing the EPR spectra to determine the rates of rotation of bound dioxygen have been developed only recently and are also reported herein.

As partner metals, to stabilize the T- and R-state conformations, we chose Fe(II) to stabilize the R state in $[\alpha_2(FeO_2)\beta_2(CoO_2)]$ and $[\alpha_2(CoO_2)\beta_2CoO_2)]$ hybrids and Zn(II) to stabilize the T state in $[\alpha_2(Zn)\beta_2(CoO_2)]$ and $[\alpha_2(CoO_2)\beta_2(Zn)]$ hybrids. Zn(II) hemoglobin has previously been shown to be in the T state,[12] and, of course, Zn(II) does not bind O_2. With foresight we might have chosen as the T-state models the Ni(II) complexes rather than Zn(II), but the extensive studies of (Ni,Fe) hybrid hemoglobins[9,35−38] that show the strong stabilization of the T-state conformation were not available when the experimental part of this work was carried out. For the Zn(II) hybrids that we have studied, we find that one of the T-state hybrids, $[\alpha_2(Zn)\beta_2(CoO_2)]$, is unique in having much slower rotation of dioxygen about the Co−O_2 bond than do the other three hybrids.

Experimental Section

General Techniques. All organic solvents and reagents not described in the following were purchased from Aldrich, E. M. Scientific, Sigma, or Mallinckrodt. TPPCo(II) and its *N*-methylimidazole (*N*-MeIm) and dioxygen adducts were prepared as described previously.[27,31]

Hybrid Hemoglobins. Unless otherwise stated, the following procedures were carried out at 6−8 °C. The heme-free form of human hemoglobin A (Sigma, 0.3−0.5 mM in heme site), hereafter called apoHb, was prepared by a modification of the acid−butanone method.[13] The changes in the procedure are as follows. Following heme removal at pH 3.0 the apoprotein solution was dialyzed 12 times against ice-cold distilled water for 20 min each followed by two dialyses, 45 min each, versus 4 °C buffer (50 mM bis-Tris, pH 8.0 for CoHb preparation, and 10 mM bis-Tris, pH 6.65 for ZnHb preparation). The solution was then dialyzed overnight against 50 mM bis-Tris, pH 8.0 for CoHb, and 10 mM bis-Tris, pH 6.65 for ZnHb. The absorption spectrum of the globin is that of a typical protein spectrum with a band centered at 280 nm; the ϵ_{mM} at 280 nm is 12.7 for human apoHb,[39] and we have used this value for determining protein concentrations in the reconstitution procedures below.

Reconstitution. *ZnHb*:[40] Globin solution, pH 6.65, 10 mM bis-Tris, was cooled to 0 °C with ice. A 1.1 equivalent amount of Zn(II) protoporphyrin (Zn(II)Por) was dissolved in a minimum amount of 0.1 N KOH (0.5−1.0 mL), diluted 10-fold with distilled water, and also chilled. The Zn(II)Por solution was added dropwise to the gently stirring globin solution (0 °C); the pH rose but was maintained between 8 and 9 by addition of dilute 4 °C HCl. After the addition of Zn(II)Por the solution

was left to stir for 1 h at 0 °C. A small amount of precipitate formed and was removed by centrifugation at 10 000 rpm for 1 min.

The supernatant was cooled to 4 °C, titrated with dilute 4 °C HCl to pH 6.65 and applied to a 1.5 × 5 column packed to a height of 3 cm with CM-trisacryl (LKB) which was equilibrated with 10 mM bis-Tris, pH 6.65. The column was washed with the same buffer until the eluate was clear. Then ZnHb was eluted with pH 6.65, 10 mM bis-Tris, plus 0.5 M NaCl. ZnHb concentration was determined spectrophotometrically using ϵ_{mM}-(550 nm) = 8.37. The solution was stored aerobically at 4−6 °C.

Zinc protoporphyrin IX was prepared from zinc acetate and protoporphyrin IX by refluxing 100 mg of the free base and 456 mg of zinc(II) acetate tetrahydrate in 50 mL of a mixture of chloroform−methanol (4:1). The reaction was monitored by recording visible spectra of aliquots withdrawn from the reaction flask. The reaction was completed within 10 min. Upon completion, the solution was placed in a separatory funnel and washed with five 100 mL portions of distilled water and evaporated to dryness.

CoHb: CoHb was prepared from apoHb and cobalt protoporphyrin IX (Sigma) as described by Yonetani et al.[41] The reduced cobalt porphyrin in aqueous pyridine was added dropwise to gently stirring globin solution under argon at 0−5 °C. After 30 min, the reconstituted CoHb was applied to an anaerobic 6.0 × 40 cm column packed to 30 cm with Sephadex G-25 (coarse) which was equilibrated with 10 mM bis-Tris, pH 6.0, and 0.25 M NaCl. This step removes the excess dithionite and reaction products from the reconstituted protein. The concentration of oxy CoHb was obtained spectrophotometrically using $\epsilon_{mM}(422) = 120$.

Preparation of Subunit-pMB Chains. A modification of the methods of Geraci et al.[42] and Ikeda-Saito et al.[43] was used. FeHb or CoHb in the oxy form, or ZnHb (1−2 mM in Zn-substituted heme and 60−80 mL volume) was allowed to react overnight with *p*-hydroxymercuribenzoate (pMB, Sigma; 10-fold excess per Hb tetramer) at pH 6.0−6.1 in the presence of 0.25 M NaCl. When the exposed groups (−SH) in position 93(β), 112(β), and 104(α) of hemoglobin were reacted with pMB dissociation into single-chain molecules occurred almost completely.[39] The next morning the pMB−Hb solution was centrifuged at 10 000 rpm for 10 min to remove any precipitate. To obtain the α^{-pMB} subunits, one-half of the solution was first applied to a 4.5 × 30 cm column packed to 25 cm with Sephadex G-25 (coarse), which was equilibrated with 0.01 M phosphate buffer at pH 8.0. Following elution of the first red band the eluate was filtered onto a 2.6 × 40 cm column packed to 35 cm with DEAE-trisacryl (LKB) which was equilibrated with 0.01 M phosphate buffer at pH 8.0. The α^{-pMB} subunits were eluted with the same buffer.

To obtain the β^{-pMB} subunits the other half of the solution was applied to a 6.0 × 40 cm column packed to 30 cm with Sephadex G-25 (coarse) which was equilibrated with 0.01 phosphate buffer at pH 6.6. Following elution of the first red band the eluate was filtered onto a 2.6 × 40 cm column packed to 30 cm with CM-trisacryl which was equilibrated with 0.01 phosphate buffer at pH 6.6. The β-pMB subunits were eluted with the same buffer. The pMB subunits were stored aerobically for 24−48 h at 4−6 °C before pMB removal and subunit recombination.

Removal of pMB.[39] The removal of pMB and subsequent recombination of subunit chains was accomplished by the method of Ikeda-Saito et al.[39] The α^{-pMB} or β^{-pMB} chains were incubated with 20 mM dithiothreitol in the presence of 5 μM catalase for 2 h. The mixture of α^{-pMB}, dithiothreitol, and catalase was passed through a 4.5 × 30 cm column packed to 25 cm with Sephadex G-25 (coarse) which was equilibrated with 10 mM phosphate buffer, pH 6.6. The red-colored α^{-SH} fraction was loaded onto a 2.6 × 50 cm column packed to 10 cm with CM-trisacryl which was equilibrated with 10 mM phosphate buffer, pH 6.6. The α^{-SH} chains stuck at the top of the column. The column was washed with the same buffer. Following this washing the α^{-SH} chains were eluted with pH 7.4, 50 mM phosphate buffer.

The mixture of β^{-pMB} chains, dithiothreitol, and catalase was passed through a 6.0 × 40 cm column packed to 30 cm with Sephadex G-25 (coarse) which was equilibrated with pH 8.67, 50 mM tris buffer. The red-colored β^{-SH} fraction was loaded onto a 1.6 × 30 cm column packed to 7 cm with DEAE-trisacryl which was equilibrated with 7 mM Tris buffer, pH 8.6. The β^{-SH} chains stuck at the top of the column. The column was washed with the same buffer, and then the β^{-SH} chains were eluted with 50 mM phosphate buffer, pH 7.4. After the buffer was changed from 50 mM phosphate, pH 7.4 to 50 mM Tris, pH 7.4, the regenerated chains were stored aerobically at −60 °C.

Recombination of Subunit Chains.[39] The α^{-SH} and β^{-SH} chains were incubated with dithiothreitol (2 mg/mL) for 1 h in the presence of 10 μM catalase before recombination. The α^{-SH} chains containing one metal were mixed with a 1.2-fold excess of β^{-SH} chains containing another metal to produce the [Fe,-Co] and [Zn,Co] hybrids. After about 2 h, the mixture was passed through a 4.5 × 30 cm column packed to 25 cm with Sephadex G-25 (coarse) which was equilibrated with 10 mM phosphate buffer, pH 6.9. The mixture was then applied to a 1.6 × 30 cm column and packed to 7 cm with DEAE-trisacryl equilibrated with the same buffer. The excess β^{-SH} chains stuck to the column while the recombined tetramer eluted from the column. After the buffer was changed from 10 mM phosphate, pH 6.9 to 50 mM bis-Tris, pH 7.4 the hybrids were stored aerobically at −60 °C.

Evaluation of the Preparations. The purity of the recombined hybrids was checked by electrophoresis on a Gelman Separatic cellulose acetate (Sephapore) gel using buffer at pH 8.8. Hybrid samples [Fe,Co] and [Zn,Co] were electrophoretically compared with normal Hb A. The presence of proteins was ascertained by treating the cellulose acetate strips with Ponceau S protein stain. Comparison of the hybrid samples with the control (Hb A) showed a very similar mobility, indicating the presence of tetrameric hybrids and a satisfactory preparation.

Spectroscopy. UV−visible spectra were obtained on a Hewlett-Packard 8451A diode array spectrophotometer at 22 ± 1 °C using 1.0 cm quartz cuvettes. X-band EPR spectra of hybrid hemoglobin solutions at pH 7.4 in 50 mM bis-Tris were recorded immediately following concentration to approximately 10 mM. EPR studies of the hybrid hemoglobins were carried out on a Varian E-12 X-band spectrometer equipped with a flowing nitrogen temperature controller at San Francisco State University. Field sweep was calibrated using a Varian weak pitch sample ($g = 2.0027$) or a sample of DPPH ($g = 2.0036$). Temperature calibration was carried out using a small-gauge copper−constantan thermocouple referenced to distilled ice water. Cobalt(II)-containing hybrid hemoglobin samples were placed in thin-walled gas-permeable Teflon microtubing (Zeuss Industrial Products, 1.2 mm o.d. × 0.05 mm wall) which was folded in half and inserted into an open-ended quartz EPR sample tube. The sample tube was then placed into the microwave node in the EPR cavity. Oxygen was used as the

thermostating gas in order to maintain the hybrid hemoglobin sample saturated with oxygen throughout the experiment.[31] Q-band EPR spectra of [TPPCo(*N*-MeIm)(O_2)] in toluene glasses were obtained at 77 K at the National EPR Center in Madison, WI.

EPR Simulations

The most rigorous method for the simulation of the EPR spectra of molecules undergoing reorientational and other motions is the stochastic Liouville theory.[44,45] This approach allows one to take into account both quantum dynamics of the electron and the nuclei and classical motion of the molecule. However, the computational complexity of this approach increases considerably with the increase in the number of both classical and quantum degrees of freedom. Thus, instead of using one universal method, we have developed several simplified methods taking into account specific features of the systems of interest to this work. In particular, the complexes under consideration have very high nuclear spin, $I = {}^7/_2$, and in addition to the rotation of the molecules as a whole, there is an extra degree of internal rotation around the Co−O axis. In all complexes both g and A tensors are associated with the O−O fragment and not with the porphyrin molecule itself.[21,23]

The following types of motion (and corresponding simulation methods) were used: (1) Slow rotation of both the molecule and the O−O group (averaging over orientations). (2) Fast rotation of the O−O group around the Co−O bond, but slow motion of the molecule. (3) Arbitrary rotation of the O−O group but slow rotation of the molecule. (4) Fast rotation of the molecule (and arbitrary rotation of the O−O group).

The ranges of applicability of some of these particular cases overlap and several methods were used for testing the consistency of the methods.

In all methods the Hamiltonian in the magnetic field scale was used:

$$\hat{H} = \vec{S}^{\mathrm{T}}\hat{G}\vec{B} + \vec{S}^{\mathrm{T}}\hat{A}\vec{I} - \frac{g_N\beta_N}{g_e\beta}\vec{I}^{\mathrm{T}}\vec{B} \tag{1}$$

This expression is obtained by dividing the Hamiltonian in the energy scale by $g_e\beta\hbar$. In the above Hamiltonian, spin operators are dimensionless, while the tensor of hyperfine interaction and eigenvalues of (1) have the dimension of magnetic field strength. The sign T denotes transpose, all other notations have the conventional meaning. In further calculations it is assumed that

$$E^{\mathrm{e}}_{\mathrm{Zeeman}} \gg E^{\mathrm{eN}}_{\mathrm{HFI}} \gg E^{\mathrm{N}}_{\mathrm{Zeeman}} \tag{2}$$

The above condition is satisfied for the complexes under consideration. Transition energies $\Delta(\vec{B})$ (in linear magnetic field scale) were calculated up to the second order of perturbation theory.

Method 1: Slow Rotation of Both the Molecule and the O−O Group. The contribution to the spectrum for a given orientation of the external magnetic field $\vec{e}$ relative to the molecule was calculated as[46]

$$F(B) \propto \frac{P}{g_{\mathrm{eff}}} f\left(\frac{B_0 - \Delta(B\vec{e})}{b}\right) \tag{3}$$

Here f is a line-shape function (assumed to be of the Gaussian or Lorentzian type), b is the line width (in gauss), and B_0 is the resonance field:

$$B_0 = h\nu_0/g_e\beta \tag{4}$$

ν_0 is the microwave frequency, P is the transition probability:

$$P = \mathrm{Tr}(\hat{G}^2) - (\vec{e}^{\mathrm{T}}\hat{G}^4\vec{e})/g_{\mathrm{eff}}{}^2 \tag{5}$$

and g_{eff} is the effective g-factor:

$$g_{\mathrm{eff}} = \sqrt{\vec{e}^{\mathrm{T}}\hat{G}^2\vec{e}} \tag{6}$$

The total spectrum was calculated as the sum of eq 3 for different transitions averaged over magnetic field orientations.

For the averaging, two-dimensional pseudo-random numbers $\vec{\epsilon}$ uniformly distributed in the unit square were used,[47,48] so that the vector

$$\vec{e} = \begin{pmatrix} \sin\theta\cos\phi \\ \sin\theta\sin\phi \\ \cos\theta \end{pmatrix} \tag{7}$$

is uniformly distributed on a unit sphere. Here

$$\cos\theta = 2\xi_1 - 1$$
$$\phi = 2\pi\xi_2 \tag{8}$$

The number of points were 2^{13} (8192) and 2^{14} (16384).

This method for the calculation of EPR spectra was accomplished by creating a computer program for an IBM-compatible PC with visual control of the simulation. The additional broadening was performed in an interactive regime in a separate program for the post-simulation processing by convolution with the Gaussian or Lorentzian functions.

Method 2: Fast Rotation of the O−O Group around the Co−O Bond, but Slow Motion of the Molecule. For the simulations of this case, the above procedure for averaging is applied to the system with already averaged g and A tensors due to the fast rotation over the Co−O bond (axis $\vec{n}$). The new (averaged) g tensor is an axial one with the principal axis $\vec{n}$ and the value

$$g_{\parallel} = \vec{n}^{\mathrm{T}}\hat{G}\vec{n} \tag{9}$$

and two axes perpendicular to the axis of rotation and the values

$$g_{\perp} = {}^1/_2(Tr\hat{G} - \vec{n}^{\mathrm{T}}\hat{G}\vec{n}) \tag{10}$$

The same expressions are valid for the partially averaged A tensor. This type of averaging is also incorporated into the EPR simulation program.

Method 3: Arbitrary Rotation of the O−O Group but Slow Rotation of the Molecule. The simplified variant of the stochastic Liouville equation was used (in fact, it is reduced to the modified Bloch equations (spectral exchange) for transverse magnetization). The angles between the directions of the external magnetic field $\vec{e}$ and the axis of rotation $\vec{n}$ were chosen to be equally spaced:

$$\theta_k = \frac{\pi}{K}\left(k - \frac{1}{2}\right) \qquad k = 1, ..., K \tag{11}$$

for each k the number of orientations (angles of rotation ϕ) M_k were chosen proportional to the area between $k_{-1/2}$ $\theta_{k+1/2}$:

$$M_k = 2K\sin\frac{\pi}{K}\left(k - \frac{1}{2}\right) \tag{12}$$

The total number of points is

$$N \approx (4/\pi)K^2 \tag{13}$$

In the calculations $K = 64$ and 128 ($N = 5215$ and 20 860) were used.

Thus, the following equations were solved:

$$-b_\tau F_{m-1} + [i(B_0 - \Delta(\vec{B}_m) + b + 2b_\tau]F_m - b_\tau F_{m+1} = ic \tag{14}$$

with the cyclic condition

$$F_{M_k+1} = F_1 \tag{15}$$

Here b is initial line width (phase relaxation), and b_τ is the rate of jumps between adjacent orientations in the magnetic field scale. This rate can be connected with the time of jumps τ and the angular diffusion coefficient D:

$$b_\tau = \frac{B_0}{\nu_0 \tau} = \frac{B_0}{\nu_0} D\left(\frac{M_k}{2\pi}\right)^2 \tag{16}$$

where c is proportional to the longitudinal relaxation and the scanning magnetic field strength. In eq 16 the definition

$$D \equiv \frac{1}{\tau(\Delta\phi)^2} = \frac{1}{\tau}\left(\frac{2\pi}{M_k}\right)^2 \tag{17}$$

was used.

The contribution to the spectrum for a given θ_k is

$$F(\theta_k) = \frac{m=1}{M_k} \mathrm{Im}\, F^m \tag{18}$$

The total spectrum is obtained by summation over all k.

Comment on the Rate of Rotation. The angular diffusion coefficient D may be connected with the "rate" of stochastic rotation R by the following relation:

$$DT = \sigma, \qquad R \equiv \frac{1}{T} = \frac{D}{\sigma} \tag{19}$$

Here σ is a numerical constant. It was chosen in the following way: The average square of the angle as a function of time is

$$\langle\phi^2\rangle = \frac{\pi^2}{3} + 4\sum_{m=1} \frac{(-1)^m}{m^2} e^{-\mathrm{D}m^2 t} \tag{20}$$

At $Dt = \pi^2/_{10} \approx 0.986\,96$ the average angle $\langle\theta\rangle$ defined as

$$\langle\phi\rangle = \sqrt{\langle\phi^2\rangle} \tag{21}$$

reaches 0.7434 of its limiting value $\pi/\sqrt{3}$. At this point $\sqrt{2Dt}$ 0.4472π or 80.5°.

The value $\pi/10$ was chosen for σ. In this case, taking into account the definition (19), b_τ can be expressed in terms of the rate of rotation R:

$$b_\tau = \frac{B_0 R M_k^2}{\nu_0 40} \tag{22}$$

Method 4: Fast Rotation of the Molecule (and Arbitrary Rotation of the O−O Group). In this case both tensors are isotropic with the following g value and HFI constant:

$$g = {}^1/_3\mathrm{Tr}(\hat{G}), \qquad a = {}^1/_3\mathrm{Tr}(\hat{A}) \tag{23}$$

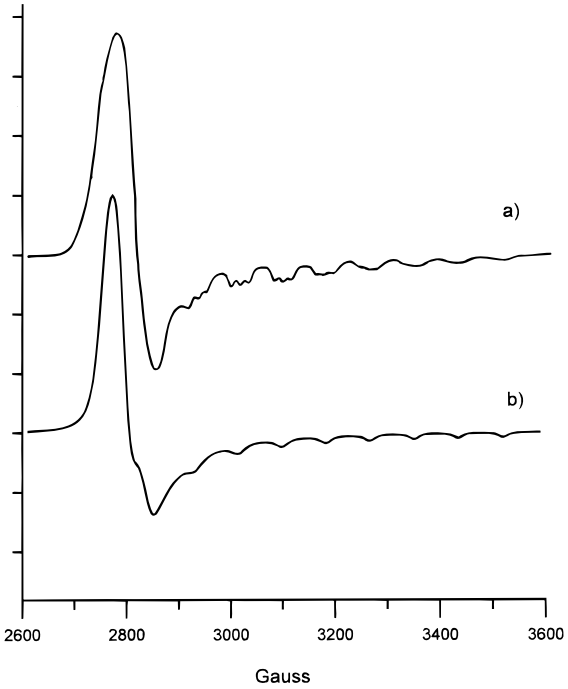

Figure 1. Experimental and simulated spectra of the 5-coordinate deoxy complex, [(*p*-OCH_3)$_4$TPPCo(Pyridine)].[27] The simulation program developed for this work does not include superhyperfine splittings.

This method was used only as a limiting case for the comparisons with the other methods.

Method 1 was first tested on the EPR spectrum of the deoxy, 5-coordinate complex [(p-OCH_3)$_4$TPPCo(pyridine)].[27] The previously reported spectrum,[27] including ^{14}N superhyperfine structure from the pyridine ligand, and the calculated spectrum, for which ^{14}N shf is not included, are compared in Figure 1. As is apparent, the simulation is quite acceptable. However, the present treatment does not properly simulate the EPR spectra having large second-order corrections, including the 4-coordinate precursor of the above-mentioned complex.[27]

Results and Discussion

EPR Experimental Results. In Figure 2 are shown the EPR spectra obtained for the four hybrid hemoglobins as a function of temperature. The resolution of the frozen spectra at 77 K (not shown) was not as good as has been reported by others,[25] because no glassing agent (methanol, ethanol, ethylene glycol, etc.) was added that might interfere with our desired study of the temperature-dependent collapse of the powder-pattern spectrum. As expected, and as can be seen, the "wings" of the glassy EPR spectrum (marked by arrows) move inward as the temperature is increased (Figure 2). Zn(II)-containing hybrid hemoglobins readily developed a free radical signal, likely from the creation of protoporphyrinatozinc(II) cation radicals and $O_2^{\bullet-}$ due to electron transfer from the zinc porphyrin to Co−O_2 centers or to O_2 itself, that became significant above temperatures of −5 °C. Even in the presence of this interfering free radical signal, the trend toward collapse of the "glassy" EPR signal as the temperature is raised is clearly evident. Spectra were analyzed qualitatively as shown in Figure 3, where the distance between the half-rise of the derivative Co−O_2 EPR signal at low-field and the half-fall of the same signal at high field was measured and defined as ΔH, a qualitative measure of "the progress toward averaging" of the EPR signal. This "progress toward averaging" is plotted as a function of temperature above the freezing point of water in Figure 4 for each of the hybrid hemoglobins studied. As is apparent from Figure

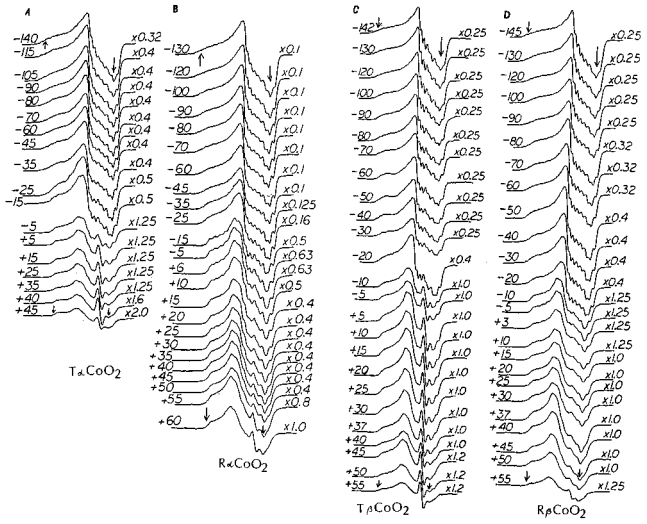

Figure 2. X-band EPR spectra of hybrid hemoglobins in 50 mM bis-Tris at pH 7.4 in the presence of 1 atm of O_2, recorded as a function of temperature: (left to right) (A) $[\alpha_2(CoO_2)\beta_2(Zn)]$, (B) $[\alpha_2(CoO_2)\beta_2(FeO_2)]$, (C) $[\alpha_2(Zn)\beta_2(CoO_2)]$, (D) $[\alpha_2(FeO_2)\beta_2(CoO_2)]$. The sharp peak centered in the "perpendicular region" of the spectra of the [Zn,Co] hybrids (A and C) is absent when zinc is absent or when the sample has not been exposed to oxygen for long periods of time, and is believed to be due to $ZnP^{+\bullet}$ and/or $O_2^{-\bullet}$, both of which can be formed by electron transfer from ZnP to O_2. The arrows on either end of the spectrum indicate the approximate starting and ending points of the spectrum and the fact that they move inward as the temperature is raised; the method used for measuring these points is shown in Figure 3.

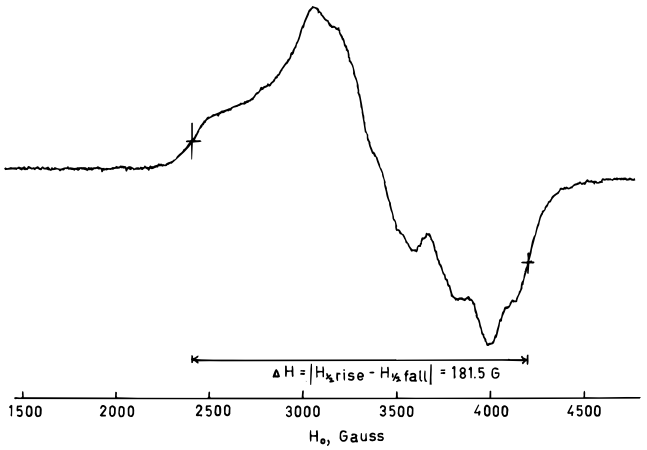

Figure 3. Enlargement of the EPR spectrum of $[\alpha_2(CoO_2)\beta_2(FeO_2)]$ at 40 °C, illustrating the method of measurement of ΔH, the "progress toward averaging" of the EPR signal: The points of half-rise and half-fall of the EPR signal were chosen as the most accurately measureable features of these cw spectra. Experimental error in this measurement is estimated to be ±2 G or less.

4, the "progress toward averaging" is reasonably linear and of similar slope in all cases, although we have refrained from fitting the data to a straight line, because the complex behavior of EPR line shapes when undergoing dynamic averaging, while they may be appear to be linear over some temperature ranges, are not in general expected to vary linearly with temperature. It can be seen that three of the hybrid hemoglobins behave similarly while the EPR signal of one is offset from the other three and thus averages more slowly. The two R-state models, $[\alpha_2(FeO_2)\beta_2(CoO_2)]$ and $[\alpha_2(CoO_2)\beta_2(FeO_2)]$, as well as one of the T-state models, $[\alpha_2(CoO_2)\beta_2(Zn)]$, all show very similar progress toward averaging as a function of temperature, while the Co−O_2 EPR signal of the fourth hybrid, $[\alpha_2(Zn)\beta_2(CoO_2)]$, is retarded in the degree of averaging at any given temperature. This is consistent with the findings of Perutz and co-workers,

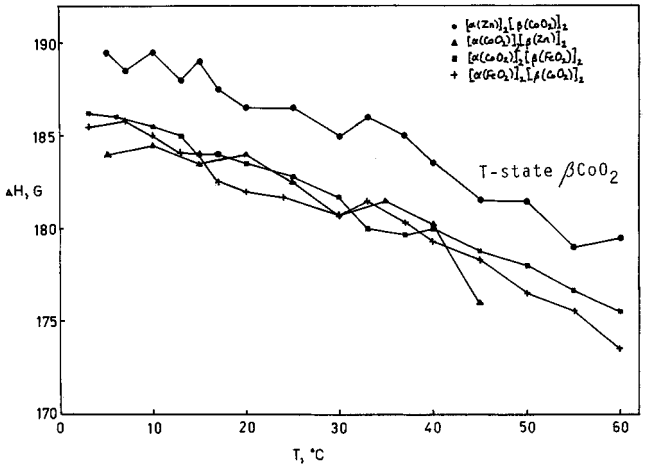

Figure 4. "Progress toward averaging", ΔH, of the CoO_2 signal as a function of temperature above the freezing point of the solvent for the four hybrids of this study, measured by the method shown in Figure 3. Note that the T-state β-chain CoO_2 signal is uniquely retarded in averaging as compared to the other three.

that the distal valine E11 blocks the binding site of O_2 in hemoglobin T-state β-chains;[9] if it blocks the binding, it must certainly block the rotation of O_2 about the Co−O_2 bond. Hence, the retardation in the "progress toward averaging" for this hybrid is consistent with steric hindrance from the distal valine E11;[9] it is not consistent with stronger H-bonding from the distal histidine to the O_2 of this hybrid than for the others,[49] since no H-bonding between the distal histidine and O_2 has been detected by X-ray crystallography for the β-chains of HbO_2.[50]

EPR Spectral Simulation Results: Estimation of the Rate of Rotation of Dioxygen. Because of better resolution in frozen toluene solvent, we have chosen to estimate the rates of rotation of dioxygen to which the EPR spectrum is sensitive by using the glassy EPR parameters of the toluene-soluble tetraphenylporphyrinatocobalt(II) *N*-methylimidazole dioxygen complex, [TPPCo(*N*-MeIm)(O_2)], rather than the hybrid hemoglobins. However, because of the extreme similarity of the EPR signals of cobalt heme−dioxygen species, the rates estimated using this model heme are expected to be very similar to those of the Co-containing hybrid hemoglobins of Figures 1−3; we are thus overlooking the very minor differences in EPR parameters reported for T- and R-state $CoHbO_2$ centers.[26]

The EPR spectrum of [TPPCo(*N*-MeIm)(O_2)] at Q-band is shown in Figure 5, together with the simulation of this spectrum. As in the case of the EPR spectrum of the deoxy complex shown in Figure 1, the simulation is quite good, with the main differences being the widths of each of the branches of the spectrum. Because of the large *g*-value dispersion at Q-band, it is possible to clearly discern the three *g* values and to estimate the hyperfine coupling constants (even though two are not resolved at this frequency). Tests of these values on the X-band EPR spectrum shown in Figure 6 confirm the values of the hyperfine coupling constants that are not resolved at Q-band. We have defined the three branches of the rhombic spectrum in the order 2, 1, and 3 from low-field to high-field end, indicating, in agreement with the structures of model hemes[32,33] and the single-crystal EPR results of Chien and Dickenson,[21] that the middle *g* value, g_1, is aligned along the O−O bond at an angle of 35° to the normal to the porphyrin plane. The high-field part of the derivative spectrum is difficult to simulate precisely because of extensive overlap between the g_1 and g_3 branches; in particular the "intensity" of the highest-field derivative line is not reproduced by the simulation, nor are the unresolved features in the 3370−3400 G region of the experi-

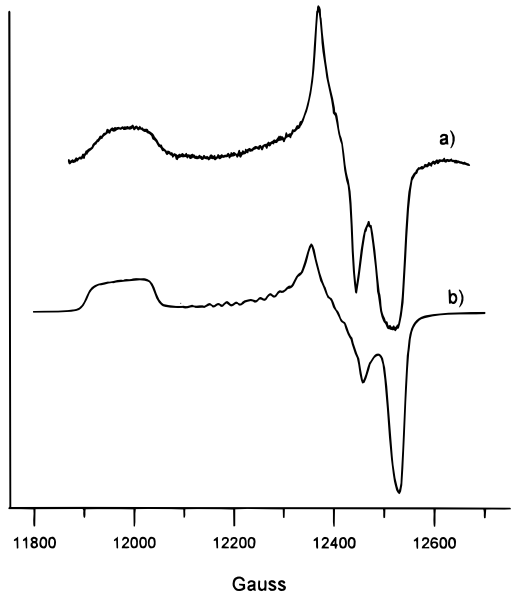

Figure 5. (a) Q-band EPR spectrum of [TPPCo(N-MeIm)(O_2)] in a toluene glass at 77 K. (b) Simulation of this spectrum using the parameters listed in Table 1.

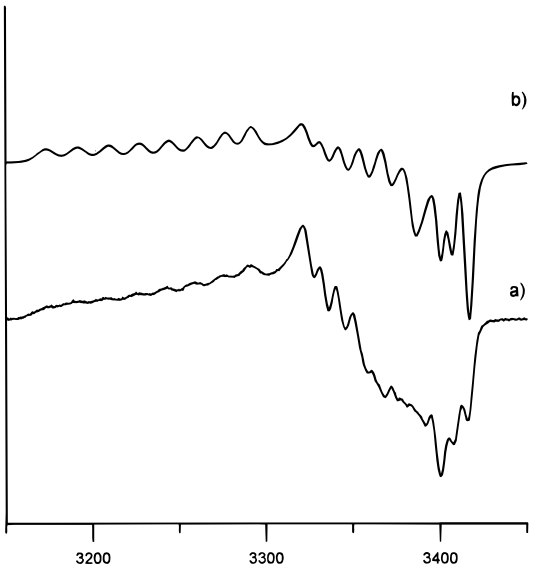

Figure 6. (a) X-band EPR spectrum of [TPPCo(N-MeIm)(O_2)] in toluene at 77 K. (b) simulation of this spectrum using the parameters listed in Table 1.

mental spectrum of Figure 6. Nevertheless, the line spacings and positions of the first and last lines are well reproduced. The best values of the *g*- and *A*-tensor components obtained from the simulations at Q- and X-band are shown in Table 1, first entry. As is apparent from the data of Table 1, the EPR parameters of the model heme complex are well within range of those reported from the single-crystal EPR data of CoMbO$_2$.[21,22] It should be noted that because of the 35° angle of g_1 to the normal to the porphyrin plane, "apparant" *a* values of polycrystalline or frozen samples reported previously are smaller (∼17−18 G for a_2)[19,27,31] than those determined using this angular relationship in the simulations, or those determined from single-crystal EPR studies.[21−23]

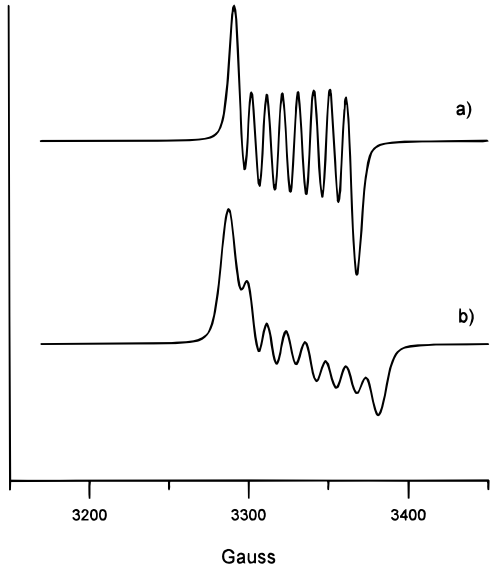

Figure 7. Simulated EPR spectra for Co−O_2 centers assuming (a) fast isotropic rotation of the entire molecule and (b) slow isotropic rotation of the entire molecule but fast rotation about the Co−O bond, where the middle *g* value is aligned along the O−O bond at an angle of 35° to the normal of the heme plane.

The *z*-axis of the *g* tensor of the Co−O_2 complex, which is aligned along the O−O bond vector, the middle *g* value,[21−23] is thus inclined at an angle of about 35° to the axis of rotation about the Co−O_2 bond. The *g* and hyperfine tensors are also noncoincident, with the same 35° angle relating g_{zz} and A_{zz}.[21] Using these results, in Figure 7 the calculated spectra obtained for the condition of fast rotation about the Co−O_2 bond (the *molecular z*-axis) and fast isotropic rotation of the entire molecule are compared. As is clear from the two curves of Figure 7, the resulting spectra are qualitatively similar but have different separations of lines, with fast rotation about the molecular *z*-axis creating a somewhat wider spacing of hyperfine lines and a difference in the broadening of the spectrum at the two ends. The latter features can be seen in the −81 to −61 °C spectra of the left-hand side of Figure 1 of ref 31, but at higher temperatures the eight-line pattern of the model cobalt heme O_2 complex is symmetrical, suggesting isotropic averaging. This 3-dimensional, isotropic averaging due to rapid molecular tumbling requires that the rotational correlation time τ_c be short compared to the inverse of the microwave frequency in angular units, or $\omega\tau_c \ll 1$,[51,52,53] and we have shown that even for the small model complexes of ref 31, it is only at or above room temperature in toluene solution that the rotational correlation time is short enough to produce complete isotropic averaging of the EPR signal.[31] This is made all the more clear

TABLE 1: EPR Parameters Obtained from Q- and X-band EPR Spectral Simulations of [TPPCo(*N*-MeIm)(O_2)] in a Toluene Glass and Comparison to Literature Values for the Co−O_2 Center of Cobalt-Substituted Myoglobin

complex	Θ[a] (deg)	g_1	g_2	g_3	a_1 (G)	a_2 (G)	a_3 (G)	⟨a⟩[b] (G)	⟨g⟩[b]	ref
[TPPCo(*N*-MeIm)(O_2)]	35[c]	2.004	2.083	1.985	4.6	21.5	3.8	10.0	2.022	TW[d]
CoMbO_2, species 1	35	2.00	2.081	1.99	13.1	23.5	8.8	15.1	2.023	21
	21	2.03	2.08	1.98	7.2	23.2	11.6	14.0	2.03	22
CoMbO_2, species 2	35	2.006	2.083	1.989	9.33	16.7	5.95	10.7	2.026	21
	17	2.008	2.085	1.983	8.2	17.3	7.2	10.9	2.025	22

[a] Angle between the normal to the heme plane and the O−O bond vector. [b] Calculated by averaging the powder pattern parameters. [c] Angle assumed for the spectral simulations of Figures 5-8. [d] This work.

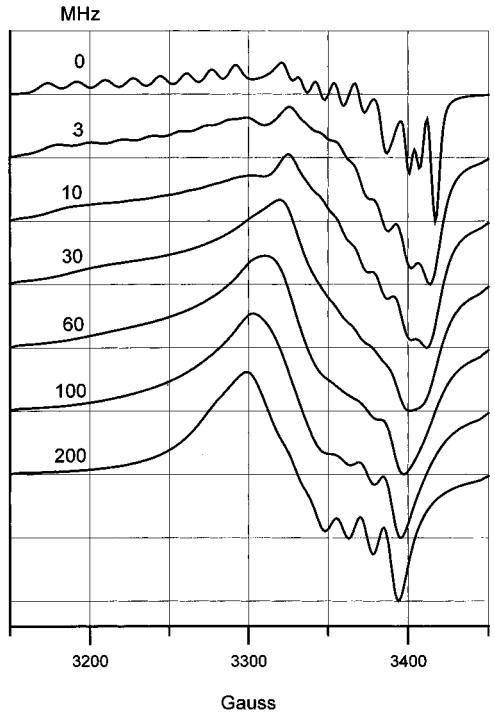

Figure 8. Simulated EPR spectra for $Co-O_2$ centers assuming rates of rotation about the Co−O bond of 3−200 MHz. Note the strong similarity of this series of calculated spectra to those of the model complex shown on the right side of Figure 1 of ref 31 as well as to the hybrid hemoglobin samples of Figure 2.

by comparison of the left- and right-hand panels of Figure 1 of ref 31, where the hydrogen-bonded $Co-O-O\cdots HNCOCH_3$ structure prevents fast rotation about the $Co-O_2$ bond of the ortho-substituted isomer. For the hybrid hemoglobins, whose rotational correlation times are at least a factor of 100 longer, isotropic averaging on the EPR time scale cannot occur at any temperature studied. This prediction is consistent with the spectra of these protein samples obtained at temperatures as high as +60 °C, which still look qualitatively similar to broadened powder patterns (Figure 2).

In Figure 8 are shown spectral simulations of the $Co-O_2$ center for varying (slow) rates of rotation about the $Co-O_2$ bond. As was observed for both the model compounds of ref 31 and the hybrid hemoglobins of Figure 2, as the rate of rotation increases the first observation is a loss of ^{59}Co hyperfine structure on the low-field end of the spectrum (3 MHz), followed by loss of the high-field hyperfine structure (30−60 MHz), and a simultaneous movement of both the low-field and high-field extrema (ΔH of Figures 3 and 4) toward the center (3−100 MHz), and finally, at quite high rates of rotation (200 MHz), the emergence of the (broadened) eight-line pattern, which is broader on the low-field end. This is qualitatively the same as the series of changes that occurred to the hydrogen-bonded model complex of the right-hand panel of Figure 1 of ref 31, and we can estimate that at −61 °C the rate of rotation of dioxygen in this hydrogen-bonded CoO_2 complex, [(*o*-$NHCOCH_3$)TPPCo(*N*-MeIm)(O_2)], is approximately 30 MHz ($\sim 3 \times 10^7$ s^{-1}). For the hybrid hemoglobins of Figure 2 we can estimate that at 35−37 °C dioxygen bound to three of the hybrids is rotating at a rate of about 100 MHz ($\sim 1 \times 10^8$ s^{-1}), while for the T-state $\beta(CoO_2)$ centers the rate is about one-third that value. The potential effect of the hydrogen-bond between N_ϵ of the distal HisE7 and the terminal oxygen atom in the α- but not the β-chains seen in the crystal structure of HbO_2[50] on the rate of rotation of bound O_2 is not specifically detectable in these measurements; the similarity in the "progress toward averaging" for both $\alpha(CoO_2)$ and one $\beta(CoO_2)$ centers, however, argues that such hydrogen-bonding may not be significant at ambient temperatures. Although more stable state-of-the-art EPR spectrometers with digital data storage would allow accurate fitting of the experimental and calculated spectra, these qualitative estimates have already provided us with new insight into the dynamics of bound dioxygen in the heme pocket of cobalt-substituted hemoglobin. The idea of dioxygen rotating at a rate of $\sim 10^8$ s^{-1} while bound in the distal pocket to the metal center of hemoglobin is certainly a concept different from that provided by the static structure of HbO_2![50]

Acknowledgment. The support of the National Institutes of Health, Grant DK-31038, and the University of Arizona Materials Characterization Program are gratefully acknowledged. The authors wish to thank the personnel at the National EPR Center for the use of their facilities for obtaining the Q-band EPR spectrum of [TPPCo(*N*-MeIm)(O_2)]. F.A.W. wishes to thank Professor Daniel Kivelson for the inspiration he provided while she was an NIH Postdoctoral Associate in his laboratory in 1966−67, where the first EPR spectrum of [TPPCo(N-MeIm)(O_2)] was recorded.

References and Notes

(1) Pertuz, M. F.; Muirhead, H.; Cox, J. M.; Goaman, L. C. G.; Mathews, F. S.; McGandy, E. L.; Webb, L. E. *Nature* **1968**, *219*, 29.
(2) Gibson, Q. H. *Prog. Biophys. Biophys. Chem.* **1956**, *9*, 1.
(3) Imai, K. *Allosteric Effects in Haemoglobin*; Cambridge University Press: Cambridge, 1982.
(4) Gibson, Q. H. *J. Biol. Chem.* **1989**, *264*, 20155.
(5) Ackers, G. K.; Doyle, M. L.; Myers, D.; Daugherty, M. A. *Science* **1992**, *255*, 54 and references therein.
(6) Monod, J.; Wyman, J.; Changeaux, J. P. *J. Mol. Biol.* **1965**, *12*, 88.
(7) Perutz, M. F. *Nature* **1970**, *228*, 726.
(8) Perutz, M. F. *Proc. R. Soc. London Ser. B* **1980**, *208*, 135.
(9) Perutz, M. F.; Fermi, G.; Luisi, B.; Shaanan, B.; Liddington, R. C. *Acc. Chem. Res.* **1987**, *20*, 309.
(10) Schlichting, I.; Berendzen, J.; Phillips, G. N.; Sweet, R. M. *Nature* **1994**, *371*, 808.
(11) Šrajer, V.; Teng, T.; Ursby, T.; Pradervand, C.; Ren, Z.; Adachi, S.; Shildkamp, W.; Bourgeois, D.; Wulff, M.; Moffat, K. *Science* **1996**, *274*, 1726.
(12) Hoffman, B. M. In *The Porphyrins*; Dolphin, D., Ed.; Academic Press: New York, 1979; Vol. 7, pp 403−472.
(13) Yonetani, T. *J. Biol. Chem.* **1967**, *242*, 5008.
(14) Teale, F. W. J. *Biochim. Biophys. Acta* **1959**, *35*, 543.
(15) Enoki, Y.; Tomita, S. *J. Mol. Biol.* **1968**, *32*, 121.
(16) Haber, J. E.; Koshland, D. E. *Biochim. Biophys. Acta* **1969**, *194*, 339.
(17) Banerjee, R.; Cassoly, R. *J. Mol. Biol.* **1969**, *42*, 351.
(18) Waterman, M. R.; Yonetani, T. *J. Biol. Chem.* **1970**, *245*, 5847.
(19) Hoffman, B. M.; Petering, D. H. *Proc. Natl. Acad. Sci. U.S.A.* **1970**, *67*, 637.
(20) Ikeda-Saito, M.; Yamamoto, H.; Yonetani, T. *J. Biol. Chem.* **1977**, *252*, 8639.
(21) Chien, J. C. W.; Dickenson, L. C. *Proc. Natl. Acad. Sci. U.S.A.* **1972**, *69*, 2783.
(22) Hori, H.; Ikeda-Saito, M.; Yonetani, T. *Nature* **1980**, *288*, 501.
(23) Dickenson, L. C.; Chien, J. C. W. *Proc. Natl. Acad. Sci. U.S.A.* **1980**, *77*, 1235.
(24) Hori, H.; Ikeda-Saito, M.; Yonetani, T. *J. Biol. Chem.* **1982**, *257*, 3636.
(25) Hori, H.; Ikeda-Saito, M.; Froncisz, W.; Yonetani, T. *J. Biol. Chem.* **1983**, *258*, 12368.
(26) Inubushi, T.; Yonetani, T. *Biochemistry* **1983**, *22*, 1894.
(27) Walker, F. A. *J. Am. Chem. Soc.* **1970**, *92*, 4235.
(28) Walker, F. A. *J. Am. Chem. Soc.* **1973**, *95*, 1154, 7928.
(29) Walker, F. A. *J. Magn. Reson.* **1974**, *15*, 201.
(30) Walker, F. A.; Beroiz, D.; Kadish, K. M. *J. Am. Chem. Soc.* **1976**, *98*, 3484.
(31) Walker, F. A.; Bowen, J. H. *J. Am. Chem. Soc.* **1985**, *107*, 8639.
(32) Lauher, R. G.; Ibers, J. A. *J. Am. Chem. Soc.* **1974**, *96*, 4447.
(33) Collman, J. P.; Gagne, R. R.; Reed, C. A.; Halbert, T. R.; Lang, G.; Robinson, W. T. *J. Am. Chem. Soc.* **1975**, *97*, 1427.

(34) Bowen, J. H. M.S. Thesis, San Francisco State University, 1987.
(35) Shelnutt, J. A.; Alston, K.; Ho, J.-Y.; Yu, N.-T.; Yamamoto, T.; Rifkind, J. M. *Biochemistry* **1986**, *25*, 620.
(36) Shibayama, N.; Inubishi, T.; Morimoto, H.; Yonetani, T. *Biochemistry* **1987**, *26*, 2194.
(37) Shibayama, N.; Imai, K.; Morimoto, H.; Saigo, S. *Biochemistry* **1993**, *32*, 8792.
(38) Shibayama, N.; Yonetani, T.; Regan, R. M.; Gibson, Q. H. *Biochemistry* **1995**, *34*, 14658.
(39) Ikeda-Saito, M.; Inubushi, T.; Yonetani, T. In *Methods in Enzymology*; Antonini, E., Rossi-Bernardi, L., Chiancone, E., Eds.; Academic Press: New York, 1981; Vol. 76, pp 113−120.
(40) Scholler, D. M.; Wang, M. R.; Hoffman, B. M. *Methods in Enzymology*; Fleischer, S., Parker, L., Eds.; Academic Press: New York, 1978; Vol. 52C, pp 487−492.
(41) Yonetani, T.; Yamamoto, H.; Woodrow, G. V. *J. Biol. Chem.* **1974**, *249*, 682.
(42) Geraci, G.; Parkhurst, L. J.; Gibson, Q. H. *J. Biol. Chem.* **1969**, *244*, 4664.
(43) Ikeda-Saito, M.; Yamamoto, H.; Imai, K.; Kayne, F. J.; Yonetani, T. *J. Biol. Chem.* **1977**, *252*, 620.
(44) Freed, J. H. Theory of Slow Tumbling ESR Spectra for Nitroxides. In *Spin Labeling: Theory and Applications*; Berliner, L., Ed.; Academic Press: New York, 1976; Vol. I, pp 53−132.
(45) (a) Sneider, D. J.; Freed, J. H. *Adv. Chem. Phys.* **1989**, *73*, 387−527. (b) Sneider, D. J.; Freed, J. H. Calculating Slow Motional Magnetic Resonance Spectra: A User's Guide. In *Biological Magnetic Resonance*; Berliner, L. J., Reuben, J., Eds.; Plenum Press: New York, 1989; Vol. 8, pp 1−76.
(46) Pilbrow, J. R. *Transition Ion EPR*; Clarendon Press: Oxford, 1990.
(47) Sobol, V. M. *The Numerical Monte Carlo Methods*; Mir: Moscow, 1979; p 125.
(48) Raitsimring, A. M.; Basu, P.; Shokhirev, N. V.; Enemark, J. H. *Appl. Magn. Reson.* **1995**, *9*, 173.
(49) Perutz, M. F., personal communication.
(50) Shaanan, B. *J. Mol. Biol.* **1983**, *171*, 31.
(51) Pople, J. A.; Schneider, W. G.; Bernstein, H. J. *High-Resolution Nuclear Magnetic Resonance*; McGraw-Hill: New York, 1959; pp 218−225.
(52) (a) Kivelson, D. *J. Chem. Phys.* **1960**, *33*, 1094. (b) Wilson, R.; Kivelson, D. *J. Chem. Phys.* **1966**, *44*, 154. (c) Atkins, P. W.; Kivelson, D. *J. Chem. Phys.* **1966**, *44*, 169.
(53) Freed, J. H.; Fraenkel, J. *J. Chem. Phys.* **1963**, *39*, 326.